MONITORING OZONE AND AEROSOL IN THE MARTIAN MESOSPHERE FROM MAVEN/IUVS STELLAR OCCULTATION OBSERVATIONS BETWEEN MY 32 AND 36.

A. S. Braude, F. Montmessin, L. Verdier, Z. Flimon, F. Lefevre, *LATMOS/CNRS/UVSQ/Sorbonne/Paris-Saclay, Guyancourt, France (ashwin.braude@latmos.ipsl.fr)*, **S. Gupta, S. K. Jain, N. M. Schneider, J. Deighan,** *LASP, U. Colorado, Boulder, USA*, **F. Y. Jiang, R. Yelle,** *LPL, U. Arizona, Tucson, USA*.

Introduction

In this talk, we will present vertically-resolved profiles of ozone and aerosol in the mesosphere, as retrieved from bimonthly stellar occultation campaigns carried out between MY 32 and 36 by the Imaging UltraViolet Spectrograph (IUVS) instrument on board the Mars Atmosphere and Volatile Evolution Mission (MAVEN) [1, 2]. Ozone is heavily correlated with other products of the photolysis of water vapour in the Martian atmosphere (notably HO_x) that are more difficult to sense remotely (e.g. [3, 4]) but which play a crucial role in the stability of Mars' CO_2 atmosphere. Since preliminary data from MY 32 and 33 was presented in [5] we have refined the process of filtering out false detections of ozone in the data, which has allowed us to provide more reliable vertical profiles not only of ozone number density, but also of aerosol optical depth in the middle atmosphere together with an associated Ångström coefficient that provides an approximate measurement of the size distribution of sub-micron particles (e.g. [6, 7]). In particular we wish to focus on regional variations in the data that can be decoupled from general differences in latitude, local time and season.

Data and Methods

The MAVEN probe has been in orbit around Mars since 2014. Since then, IUVS stellar occultation observation campaigns have taken place approximately once every two months, with each campaign typically consisting of roughly 50-100 individual stellar occultations optimised to provide substantial longitudinal coverage for a given latitude and solar longitude. IUVS makes use of a beam splitter to direct incoming radiation towards two separate detectors: one sensitive to the FUV (110 - 190 nm) and one to the MUV (180 - 300 nm), with a spectral sampling of 0.3 nm and 0.7 nm respectively following spectral binning. The FUV component is mostly sensitive to CO_2 and O_2 absorption above around 80 km, while the MUV component contains an ozone absorption feature at 250 nm (the 'Hartley Band') that provides information on ozone number density between approximately 20 and 60 km altitude. In addition, systematic absorption in the MUV can be used to retrieve aerosol optical depth $\tau_{(\lambda=250nm)}$ while the spectral slope α can be used to determine the approximate size distribution of small (<0.5μm) particles.

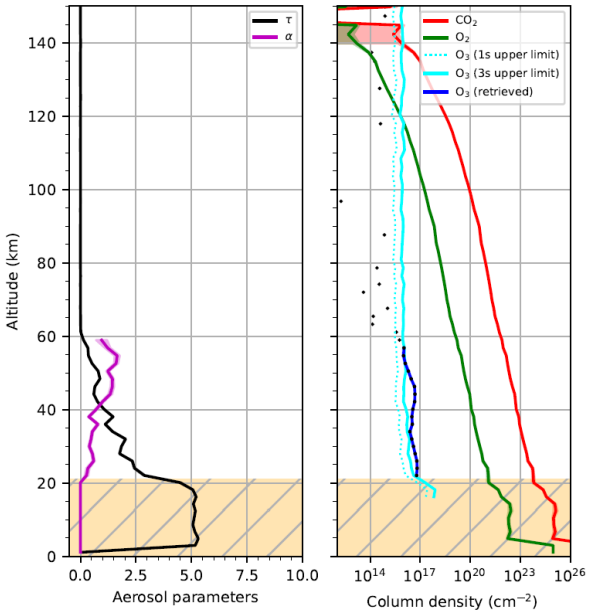

Figure 1: Example retrieval of aerosol and molecular column densities from an IUVS occultation obtained near the Equator at aphelion. Left: retrieved aerosol parameters $\tau_{(\lambda=250nm)}$ (aerosol optical depth, black) and α (Ångström coefficient, magenta). The orange cross-hatched region marks lower altitudes at which the spectra are saturated due to the presence of dust. The increase in α with altitude indicates the presence of a haze or ice cloud layer at high altitude. Right: retrieval of CO_2, O_2 and O_3 column densities. Black dots indicate individual retrieved ozone column densities. The light blue line indicates significant detections of ozone, while ozone column densities that are below the 2 sigma detection limit are discarded from the vertical inversion.

We selected 510 individual occultations in our analysis out of the 40 observation campaigns that have been processed as of writing, according to the availability of MUV data and the quality of calibration and straylight correction. In practice this also limits us to using nightside occultations where the effect of straylight on the

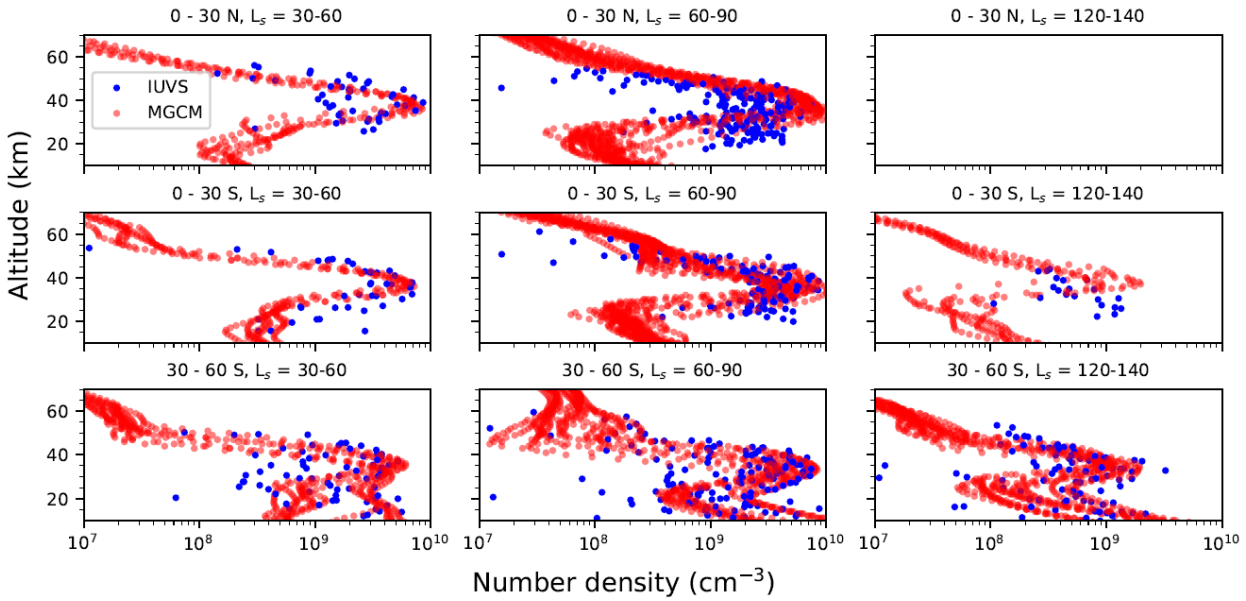

Figure 2: Comparison of vertical profiles of ozone local density at aphelion, between measurements from IUVS (blue) and modelled values from the LMD MGCM (red).

MUV due to scattered sunlight is minimised. We first perform a spectral inversion procedure in order to simultaneously retrieve vertical profiles of CO_2, O_2 and O_3 column density, together with $\tau_{(\lambda=250nm)}$ and α (Fig. 1). Variations in CO_2 and O_2 observed by IUVS are mostly only relevant to the upper atmosphere well above the altitudes at which IUVS is sensitive to ozone and aerosol, and so will be mostly beyond the scope of this talk.

Following spectral inversion, ozone upper limit values are estimated at each altitude by progressively injecting ozone column density values into the forward model until a given reduced χ^2 threshold is reached [8, 9], so that ozone detections of below 2σ significance can be rejected to minimise the number of false detections due to fitting noise or artefacts in the data. A vertical inversion procedure is then performed on the resulting column density profiles to retrieve profiles of local density of O_3.

For more details on the instrument specifications as well as the calibration, spectral and vertical inversion procedures, refer to [10, 1, 5].

Ozone - Preliminary results and perspective

We identify positive ozone detections in approximately 38% of IUVS stellar occultations, mostly concentrated around aphelion. In Fig. 2 we display some preliminary retrievals of ozone around aphelion in equatorial and mid-latitudinal regions, and compare them with corresponding profiles generated from the LMD Mars General Circulation Model (MGCM) [11]. We generally find good correspondence between the modelled and observed night-time ozone layer at around 40 km. We also retrieve a near-surface layer of ozone below 20 km altitude in the mid-latitudes where observations near the surface are less limited by the presence of aerosol. These ozone layers are generally well-attested in other measurements of ozone made both by the SPICAM and NOMAD instruments in the UV (e.g. [12, 13]), and with the ACS instrument in the mid-infrared [14]. However, we also observe more variability in altitude than is reflected in modelled ozone densities. In this talk we will further discuss differences between observed and modelled ozone profiles more broadly across the latitude and temporal range covered in this analysis, and identify their possible origins.

Aerosols - Preliminary results and perspective

The exact composition of aerosol layers cannot be directly determined from observations in the ultraviolet, but measuring vertical correlations in Ångström coefficient and temperature together with some knowledge of microphysics can provide some constraints on their morphology to first order. As was found in data from SPICAM-UV ([7, 15], we also identify a substantial number of observations featuring aerosol present in two or more discrete vertically-resolved layers (‘detached layers’), as well as some observations with mesospheric cloud layers present at very high altitude [16, 17]. We find that, like in the work of [15], the predicted decrease of Ångström coefficient with height (indicating smaller

particle radii) is common, but not universal. In this talk we will seek to characterise the general variation of aerosol with latitude and season in more detail, and map the distribution of detached aerosol layers with an additional focus on identifying regional and longitudinal variations not linked to differences in latitude, season or local time. We will also examine their impact on longitudinal variations in observations of ozone on Mars.

References

[1] W. E. McClintock, N. M. Schneider, G. M. Holsclaw, J. T. Clarke, A. C. Hoskins, I. Stewart, F. Montmessin, R. V. Yelle, J. Deighan, The Imaging Ultraviolet Spectrograph (IUVS) for the MAVEN Mission, *Space Sci. Rev.* 195 (2015) 75–124. doi:10.1007/s11214-014-0098-7.

[2] B. M. Jakosky, J. M. Grebowsky, J. G. Luhmann, D. A. Brain, Initial results from the MAVEN mission to Mars, *Geophys. Res. Lett.* 42 (2015) 8791–8802. doi:10.1002/2015GL065271.

[3] M. B. McElroy, T. M. Donahue, Stability of the Martian Atmosphere, Science 177 (1972) 986–988. doi:10.1126/science.177.4053.986.

[4] F. Lefèvre, V. Krasnopolsky, Atmospheric Photochemistry, in: R. M. Haberle, R. T. Clancy, F. Forget, M. D. Smith, R. W. Zurek (Eds.), The Atmosphere and Climate of Mars, 2017, pp. 374–404. doi:10.1017/9781139060172.013.

[5] H. Gröller, F. Montmessin, R. V. Yelle, F. Lefèvre, F. Forget, N. M. Schneider, T. T. Koskinen, J. Deighan, S. K. Jain, MAVEN/IUVS Stellar Occultation Measurements of Mars Atmospheric Structure and Composition, *J. Geophys. Res. Planets* 123 (2018) 1449–1483. doi:10.1029/2017JE005466.

[6] O. Dubovik, A. Smirnov, B. N. Holben, M. D. King, Y. J. Kaufman, T. F. Eck, I. Slutsker, Accuracy assessments of aerosol optical properties retrieved from Aerosol Robotic Network (AERONET) Sun and sky radiance measurements, *J. Geophys. Res.* 105 (2000) 9791–9806. doi:10.1029/2000JD900040.

[7] F. Montmessin, E. Quémerais, J. L. Bertaux, O. Korablev, P. Rannou, S. Lebonnois, Stellar occultations at UV wavelengths by the SPICAM instrument: Retrieval and analysis of Martian haze profiles, *J. Geophys. Res. Planets* 111 (2006) E09S09. doi:10.1029/2005JE002662.

[8] N. A. Teanby, P. G. J. Irwin, R. de Kok, A. Jolly, B. Bézard, C. A. Nixon, S. B. Calcutt, Titan's stratospheric C_2N_2, C_3H_4, and C_4H_2 abundances from Cassini/CIRS far-infrared spectra, *Icarus* 202 (2009) 620–631. doi:10.1016/j.icarus.2009.03.022.

[9] N. A. Teanby, P. G. J. Irwin, J. I. Moses, Neptune's carbon monoxide profile and phosphine upper limits from Herschel/SPIRE: Implications for interior structure and formation, *Icarus* 319 (2019) 86–98. doi:10.1016/j.icarus.2018.09.014.

[10] E. Quémerais, J.-L. Bertaux, O. Korablev, E. Dimarellis, C. Cot, B. R. Sandel, D. Fussen, Stellar occultations observed by SPICAM on Mars Express, *J. Geophys. Res. Planets* 111 (2006) E09S04. doi:10.1029/2005JE002604.

[11] F. Lefèvre, S. Lebonnois, F. Montmessin, F. Forget, Three-dimensional modeling of ozone on Mars, *J. Geophys. Res. Planets* 109 (2004) E07004. doi:10.1029/2004JE002268.

[12] S. Lebonnois, E. Quémerais, F. Montmessin, F. Lefèvre, S. Perrier, J.-L. Bertaux, F. Forget, Vertical distribution of ozone on Mars as measured by SPICAM/Mars Express using stellar occultations, *J. Geophys. Res. Planets* 111 (2006) E09S05. doi:10.1029/2005JE002643.

[13] M. R. Patel, G. Sellers, J. P. Mason, J. A. Holmes, M. A. J. Brown, S. R. Lewis, K. Rajendran, P. M. Streeter, C. Marriner, B. G. Hathi, et al., ExoMars TGO/NOMAD-UVIS Vertical Profiles of Ozone: 1. Seasonal Variation and Comparison to Water, *J. Geophys. Res. Planets* 126 (2021) e06837. doi:10.1029/2021JE006837.

[14] K. S. Olsen, F. Lefèvre, F. Montmessin, A. Trokhimovskiy, L. Baggio, A. Fedorova, J. Alday, A. Lomakin, D. A. Belyaev, A. Patrakeev, A. Shakun, O. Korablev, First detection of ozone in the mid-infrared at Mars: implications for methane detection, *A&A* 639 (2020) A141. doi:10.1051/0004-6361/202038125.

[15] A. Määttänen, C. Listowski, F. Montmessin, L. Maltagliati, A. Reberac, L. Joly, J.-L. Bertaux, A complete climatology of the aerosol vertical distribution on Mars from MEx/SPICAM UV solar occultations, *Icarus* 223 (2013) 892–941. doi:10.1016/j.icarus.2012.12.001.

[16] M. H. Stevens, D. E. Siskind, J. S. Evans, S. K. Jain, N. M. Schneider, J. Deighan, A. I. F. Stewart, M. Crismani, A. Stiepen, M. S. Chaffin, W. E. McClintock, G. M. Holsclaw, F. Lefèvre, D. Y. Lo, J. T. Clarke, F. Montmessin, B. M. Jakosky, Martian mesospheric cloud observations by IUVS on MAVEN: Thermal tides coupled to the upper atmosphere, *Geophys. Res. Lett.* 44 (2017) 4709–4715. doi:10.1002/2017GL072717.

REFERENCES

[17] F. Y. Jiang, R. V. Yelle, S. K. Jain, J. Cui, F. Montmessin, N. M. Schneider, J. Deighan, H. Gröller, L. Verdier, Detection of Mesospheric CO_2 Ice Clouds on Mars in Southern Summer, *Geophys. Res. Lett.* 46 (2019) 7962–7971. doi:10.1029/2019GL082029.